dBi at the resonance frequency. Antenna 3 provides a maximum gain of 2.2 dBi at 1.52 GHz for the CP state.

IV. Conclusion

A single feed electronically reconfigurable microstrip antenna with switchable slots for frequency and polarization diversities has been presented in this communication. The antenna can produce linear and circular polarization by controlling the bias conditions of two PIN diodes. A good impedance matching performance for all polarization states is observed without any matching networks. The proposed design achieves a cross polar level better than -10 dB in linear polarization and 1.18% CP bandwidth in circular polarization state with broadside radiation characteristics and moderate gain. In addition, the antenna is simple and compact because it uses only a few active and passive components and requires less area to occupy the patch and dc-bias circuit compared to conventional polarization diversity antennas. The frequency and polarization diversities of this design provide some potential applications for wireless communications.

References

[1] J. Mitola and G. Q. Maguire, "Cognitive radio: Making software radios more personal," *IEEE Personal Commun. Mag.*, vol. 6, no. 4, pp. 13–18, Aug. 1999.

[2] M. A. Kossel, R. Kung, H. Benedickter, and W. Bachtold, "An active tagging system using circular polarization modulation," *IEEE Trans. Microw. Theory Tech.*, vol. 47, no. 12, pp. 2242–2248, Dec. 1999.

[3] M. Boti, L. Dussopt, and J.-M. Laheurte, "Circularly polarized antenna with switchable polarization sense," *Electron. Lett.*, vol. 36, no. 18, pp. 1518–1519, Aug. 2000.

[4] F. Yang and Y. Rahmat-Samii, "A reconfigurable patch antenna using switchable slots for circular polarization diversity," *IEEE Microw. Wireless Compon. Lett.*, vol. 12, no. 3, pp. 96–98, Mar. 2002.

[5] M.-H. Ho, M.-T. Wu, C.-I. G. Hsu, and J.-Y. Sze, "An RHCP/LHCP switchable slotline-fed slot ring antenna," *Microw. Opt. Technol. Lett.*, vol. 46, no. 1, pp. 30–33, Jul. 2005.

[6] M. K. Fries, M. Grani, and R. Vahldieck, "A reconfigurable slot antenna with switchable polarization," *IEEE Microw. Wireless Compon. Lett.*, vol. 13, no. 11, pp. 490–492, Nov. 2003.

[7] Y. J. Sung, "Reconfigurable patch antenna for polarization diversity," *IEEE Trans. Antennas Propag.*, vol. 56, no. 9, pp. 3053–3054, Sep. 2008.

[8] B. Kim, B. Pan, S. Nikolaou, Y.-S. Kim, J. Papapolymerou, and M. M. Tentzeris, "A novel single-feed circular microstrip antenna with reconfigurable polarization capability," *IEEE Trans. Antennas Propag.*, vol. 56, no. 3, pp. 630–638, Mar. 2008.

[9] M. Ali, A. T. M. Sayem, and V. K. Kunda, "A reconfigurable stacked microstrip patch antenna for satellite and terrestrial links," *IEEE Trans. Antennas Propag.*, vol. 56, no. 2, pp. 426–435, Mar. 2007.

[10] S. V. Shynu, G. Augustin, C. K. Aanandan, P. Mohanan, and K. Vasudevan, "A compact electronically reconfigurable dual frequency microstrip antenna for L-band applications," *Int. J. Wireless Opt. Comm.*, vol. 2, no. 2, pp. 181–187, 2004.

[11] M. S. Nishamol, V. P. Sarin, A. Gijo, V. Deepu, C. K. Aanandan, P. Mohanan, and K. Vasudevan, "Compact dual frequency dual polarized cross patch antenna with an x-slot," *Microw. Opt. Technol. Lett.*, to be published.

A Novel Hexa-Band Antenna for Mobile Handsets Application

Chia-Mei Peng, I-Fong Chen, and Chia-Te Chien

***Abstract*—A novel hexa-band antenna for mobile handsets application is proposed and analyzed in this communication. An asymmetric T-type monopole antenna with a shorted-line is designed to be operated in code-division multiple access (CDMA, 824–894 MHz), global system for mobile communications (GSM, 880–960 MHz), digital communication system (DCS, 1710–1880 MHz), personal communication system (PCS, 1850–1990 MHz), wideband code division multiple access (WCDMA, 1920–2170 MHz) and Bluetooth (2400–2484 MHz) bands. A prototype of the proposed antenna with 50 mm in length, 3 mm in height and 15 mm in width is fabricated and experimentally investigated. The experimental results indicate that the VSWR 2.5:1 bandwidths achieved were 17.8% and 37.1% at 900 MHz and 2100 MHz, respectively. The specific absorption rate (SAR) for an input power of 24 dBm in CDMA, GSM and WCDMA bands, and an input power of 21 dBm in DCS and PCS bands all meet the SAR limit of 1.6 mW/g. Experimental results are shown to verify the validity of theoretical work.**

***Index Terms*—Hexa-band antenna, mobile handsets, shorted-line, specific absorption rate (SAR), T-type monopole.**

I. Introduction

Wireless communications continue to enjoy exponential growth in the cellular telephony, wireless Internet, and wireless home networking arenas. In order to roam worldwide, the operation bands of major wireless services, such as code-division multiple access (CDMA), global system for mobile communications (GSM), digital communication system (DCS), personal communication system (PCS), wideband code division multiple access (WCDMA) and Bluetooth should be simultaneously considered [1]. Downsizing the handset unit, which has seen remarkable progress in recent years, requires the size reduction of the antenna element also. However, as a small antenna element is used, the utilization of the handset body is beneficial to enhance antenna performance of the handset because the handset body is usually larger than the antenna element. Therefore, the overall effective antenna dimensions augment dramatically. As a consequence, the corresponding gain and the bandwidth of the antenna system are increased [2]–[10]. While the use of the handset body as a part of the radiator is advantageous, it also caused disadvantage at the same time in practical operation. The antenna performance in terms of gain and input impedance varies due to the influence of the human head and hand. In this communication, an asymmetric T-type monopole antenna is designed jointly with a solid shorting-line to achieve hexa-band

Manuscript received September 16, 2010; revised November 13, 2010; accepted January 26, 2011. Date of publication July 07, 2011; date of current version September 02, 2011. This work was supported by the National Science Council, R.O.C., under Contract 97-2221-E-228-004.

C.-M. Peng and I.-F. Chen are with the Department of Electronic Engineering and Institute of Computer and Communication Engineering, Jinwen University of Science and Technology, Taipei, Taiwan, R.O.C. (e-mail: ex0206@just.edu.tw). .

C.-T. Chien us with the Department of Electronic Engineering and Institute of Computer and Communication Engineering, Jinwen University of Science and Technology, Taipei, Taiwan, R.O.C. and also with the Department of Communication Engineering, National Chiao Tung University, Hsinchu, Taiwan, R.O.C.

Color versions of one or more of the figures in this communication are available online at http://ieeexplore.ieee.org.

Digital Object Identifier 10.1109/TAP.2011.2161447

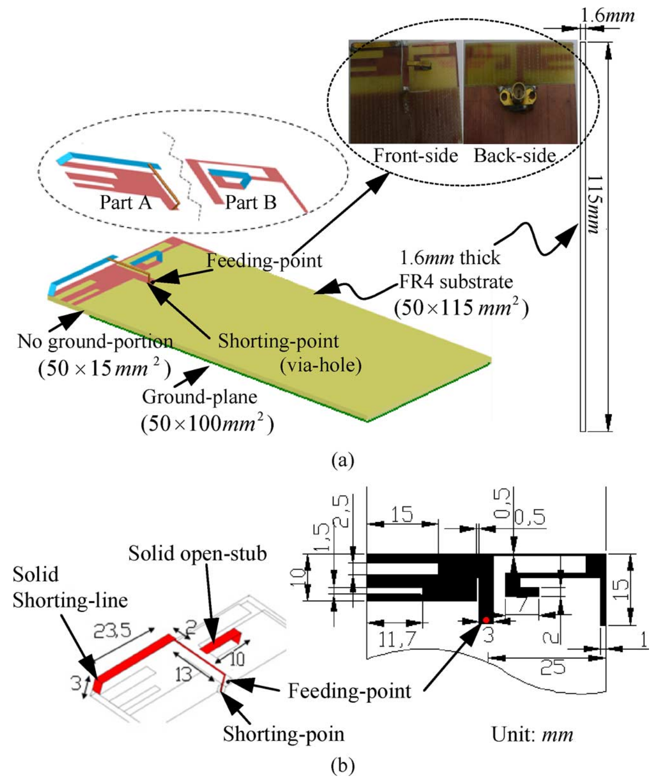

Fig. 1. (a) Geometry of the proposed antenna for hexa-band operation in the mobile handset. (b) Dimensions of the proposed antenna.

(CDMA, GSM, DCS, PCS, WCDMA and Bluetooth) performance. A hexa-band antenna is constructed to operate in the range of a dual operating-band: lower-operating band (CDMA and GSM) and upper-operating band (DCS, PCS, WCDMA and Bluetooth). The proposed antenna has a dual asymmetric radiated-strip structure that is developed by modifying the structure of a printed T-type monopole. The feasibility of wide bandwidth operation has been proven by the design of a solid shorted-line and a solid open-stub radiating structure to operate in the dual operating bands. Smaller power loss (dB absorption) due to the influence of phantom-head model is shown. It is also demonstrated that the proposed antenna structure produces a low specific absorption rate (SAR) value. Details of the design considerations and the experimental results of the constructed prototype are presented and discussed in the following sections.

II. Antenna Structure and Design

Fig. 1(a) shows the geometry of the proposed antenna for hexa-band operation in the mobile handset. The presented antenna structure is composed of an asymmetric T-type monopole which is printed on a FR4 glass epoxy substrate with the thickness of 1.6 mm, relative permittivity of 4.3 and loss tangent of 0.023. The proposed antenna is placed on a portion without metal ground on the backside. All sections are at the same layer. One of the asymmetric T-type strips combined with solid shorting-line to form a loop structure is denoted as part A. The other strip combined with solid open-stub is denoted as part B. The electrical-length of the radiating elements can be determined from the quarter-wave length at the resonant frequencies. Detailed dimensions of the proposed antenna are given in Fig. 1(b). In part A, the resonant frequency is designed to occur at 1800 MHz, the electrical-length of the planar-strip is equal to 40 mm (which is $15\ \mathrm{mm} + 25\ \mathrm{mm}$). For covering DSC, PCS, WCDMA and Bluetooth bands, the shape of part A is designed for wideband operation, the tuning of broad bandwidth is obtained by increasing strip-area and inserting some slits. These slits cause the discontinuities of the current distribution on the surface of radiating-strip which improves the impedance bandwidth [11], [12].

In part B, the resonant frequency is designed to occur at 900 MHz, the electrical-length of the planar-strip is equal to 80 mm (which is $15\ \mathrm{mm} + 25\ \mathrm{mm} + 6\ \mathrm{mm} + 22\ \mathrm{mm} + 5\ \mathrm{mm} + 7\ \mathrm{mm}$). For covering CDMA and GSM bands, the solid-open stub is used as a top-loading of part B and it increases the electrical-length and impedance bandwidth in the antenna's lower-operating band. The impedance matching at lower- and upper-operating bands can be also tuned by solid shorting-line of part A and extended strip of part B. The solid shorting-line is found to be effective in obtaining a wider impedance bandwidth in the antenna's upper-operating band. Note that the widths of these strips, slits, solid shorting-line and solid open-stub, etc., are not identical. By selecting appropriate dimensions (part A, part B) of the antenna structure, good impedance matching of the asymmetric T-type monopole can be obtained, and thus the bandwidth is also extended. Besides, [7] indicated that the ground-plane mode is responsible for SAR. Hence, in order to demonstrate the low current distribution on the handset body, the effect of varying the ground-plane length of the proposed antenna structure is investigated by simulations. Detail results will be presented and discussed in the next section.

III. Experimental Results and Discussion

In the experiment, the feeding-point and ground-plane are connected to a 50 Ω SMA connector. By using the described design procedure, a hexa-band antenna is constructed to operate in the range of a dual operating-band: lower-operating band (CDMA and GSM) and upper-operating band (DCS, PCS, WCDMA and Bluetooth). Fig. 2(a) shows the measured and simulated V.S.W.R plot of the dual band antenna and the V.S.W. $\mathrm{R} \leq 2$ bandwidths are 135 MHz (15%) and 790 MHz (37.6%) at 900 MHz and 2100 MHz, respectively. The simulated results are obtained by using the Ansoft HFSS. We can also find that a good agreement between the simulation and measurement is obtained. Fig. 2(b) shows the measured V.S.W.R of the proposed antenna in terms of part A and part B. For part A only, the radiated-strip and the shorting-line is matched at the DCS, PCS and WCDMA bands, the 560 MHz (28% at 2000 MHz) operating bandwidth is shown. This is due to the fact that the surface current distribution of the asymmetric radiated-strip is discontinuous. For part B only, the modified bended monopole antenna is matched at the GSM and PCS bands. As expected, the measured results indicate that part A and part B introduce an upper- and lower-operating band, respectively.

The measured Smith Chart as shown in Fig. 2(c), the full characteristics of the proposed antenna are shown. Fig. 3 presents the measured 3-D and 2-D radiation patterns in the free space at 850 MHz and 902 MHz in the xy-plane and yz-plane, respectively. It is obvious that the dipole-like radiation patterns are observed. In other words, at the lower-operating bands, the ground-plane becomes a part of the antenna, and is responsible for the radiation [7]. The measured radiation patterns at 1720, 1920, 2045 and 2450 MHz are shown in Fig. 4. From Fig. 4, more variations in the radiation pattern-shapes are obtained, as compared to those in Fig. 3. This is probably because the ground-plane still acts as a part of the antenna at the upper-operating band. The overall ground-plane length is about one wavelength long and there are normally four main lobes at the upper-operating band.

Table I. presents the measured antenna total efficiency of the proposed antenna in the free space (without phantom-head and phantom-hand), and with phantom-head and phantom-hand.

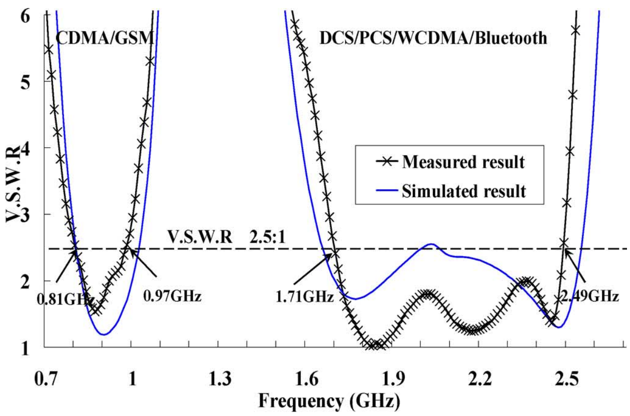

(a)

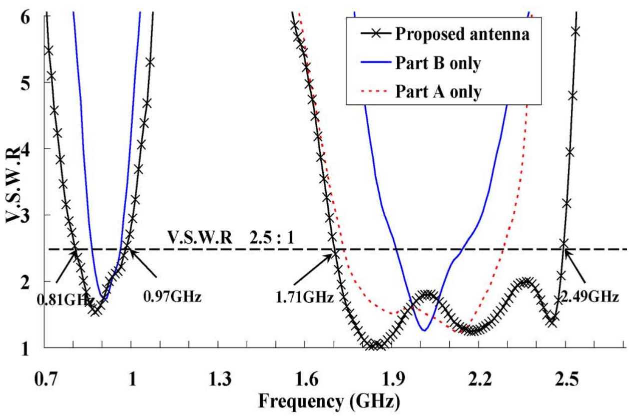

(b)

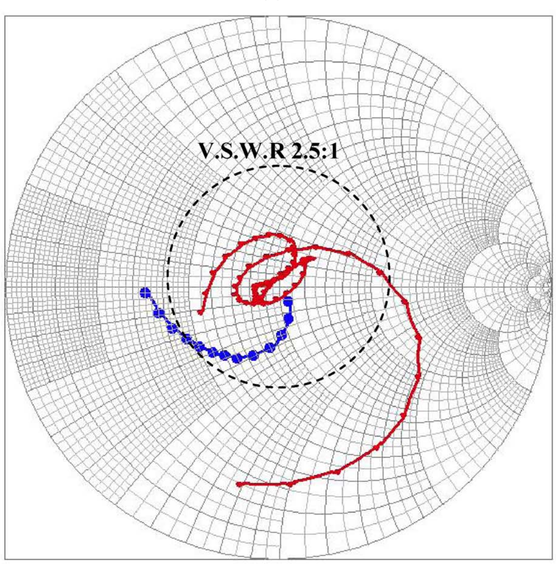

(c)

Fig. 2. (a) The measured and simulated V.S.W.R against frequency. (b) The measured V.S.W.R in terms of the part A and part B. (c) The measured Smith Chart of the proposed antenna.

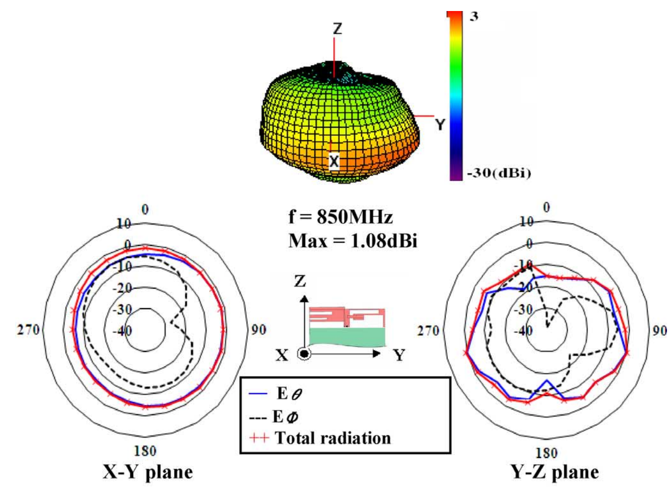

(a)

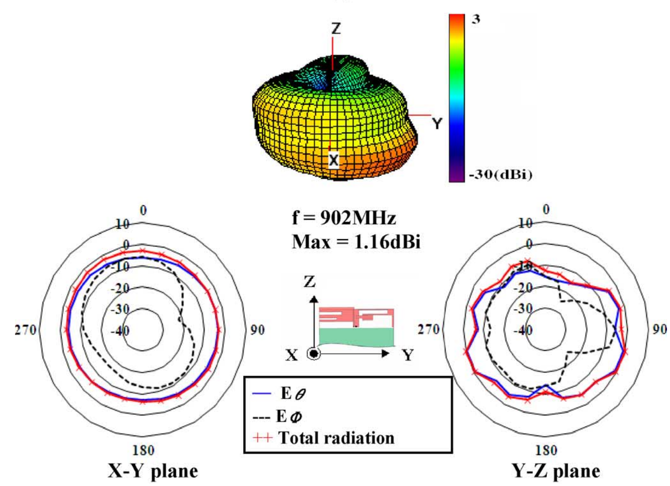

(b)

Fig. 3. Measured 3-D and 2-D radiation patterns at (a) 850 MHz and (b) 902 MHz for the proposed antenna.

Acceptable radiation characteristic for the practical applications is obtained for the proposed antenna. The omni-directional feature of the proposed antenna can be observed from the Horizontal-plane. The effect of the proposed antenna structure on the antenna performance is also studied and the results are described below. In addition, the SAR results of the proposed antenna are also analyzed.

A. Analysis of the Proposed Antenna Structure

The design parameters and the corresponding characteristics of the resonant frequency, input impedance and bandwidth are a function of the geometrical parameters of the proposed antenna. The simulated current distribution of the proposed antenna structure on the handset body is shown in Fig. 5. In the upper-operating band, only a few current is distributed on the handset body. Note that a small loop antenna can be regarded as a magnetic dipole normal to the loop plane and it reduces the current flow on the handset body [6], [7]. However, in the lower-operating band, more current are distributed on the handset body as compared to those in the upper-operating band. That is because in the lower-operating band, the electrical-length of the modified bended monopole is over one quarter-wavelength, as a consequently, the input impedance of the modified bended monopole is matched to the handset body [3]–[7]. When a mobile handset is used in close proximity to a human head, dielectric-loading effect can be expected, there may also be a detuning issue. In order to demonstrate the distinctive performance of the proposed antenna in the presence of a human head, the measurement efficiency set-up with the phantom-head is shown in Fig. 6. The liquid parameters used in the measurements are listed in Table II. The measured V.S.W.R against frequency of antenna with phantom-head is shown in Fig. 7.

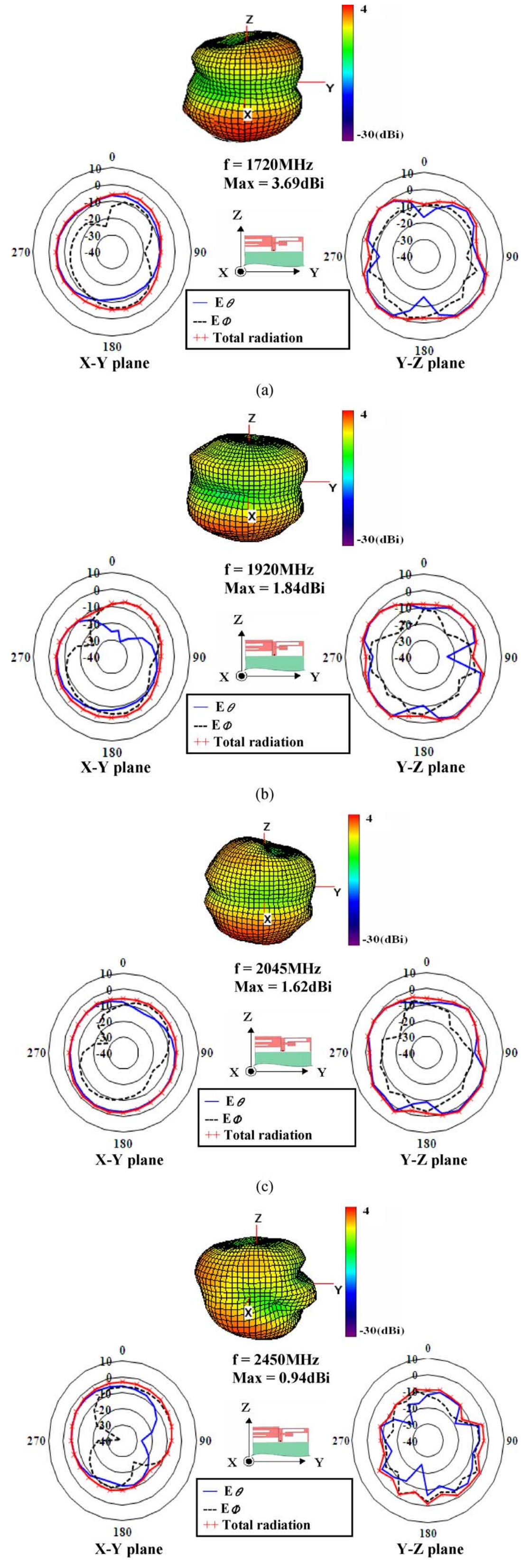

Fig. 4. Measured 3-D and 2-D radiation patterns at (a) 1720 MHz, (b) 1920 MHz, (c) 2045 MHz, (d) 2450 MHz for the proposed antenna.

The degradation of total efficiency of antenna with phantom-head is shown in Table I.

TABLE I
THE MEASURED ANTENNA GAINS AND THE TOTAL EFFICIENCY WITHIN THE OPERATING BANDWIDTH OF THE PROPOSED ANTENNA

Frequency (MHz)	Efficiency (%) (Antenna in free space)	Efficiency (%) (Antenna with phantom head)	Loss (dB) (Antenna with phantom head)	Efficiency (%) (Antenna with phantom hand)	Loss (dB) (Antenna with phantom hand)
850	60.23	23.61	4.07	33.15	2.59
902	61.47	25.51	3.82	33.41	2.65
1720	64.21	27.43	3.69	30.39	3.25
1920	68.11	27.91	3.87	31.74	3.32
2045	71.44	26.53	4.30	38.02	2.74
2450	68.73	25.67	4.28	35.83	2.83

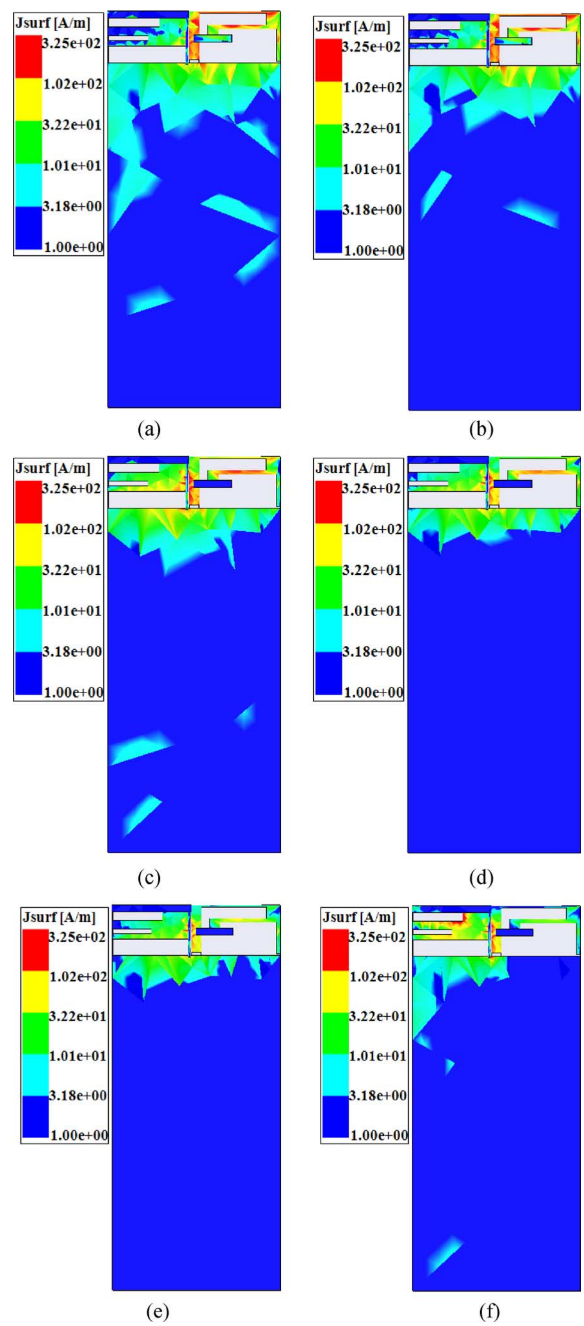

Fig. 5. The simulated current distribution of the proposed antenna structure on the handset body (the ground-length is 100 mm) at (a) 850 MHz, (b) 902 MHz, (c) 1720 MHz, (d) 1920 MHz, (e) 2045 MHz, (f) 2450 MHz.

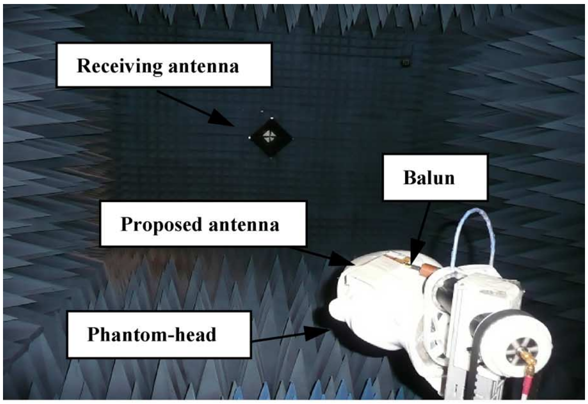

(a)

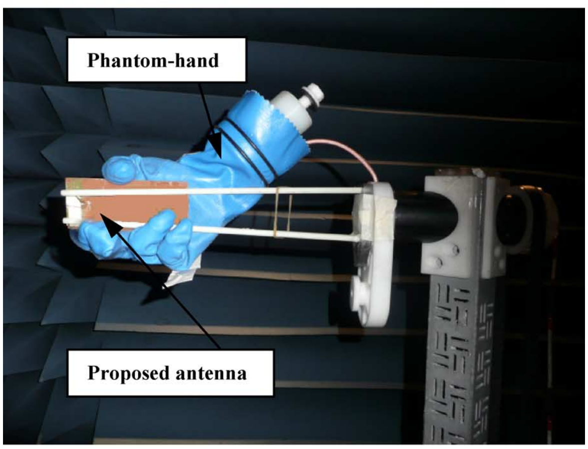

(b)

Fig. 6. Photo of experimental arrangement for efficiency measurement with (a) Phantom-head. (b) Phantom-hand.

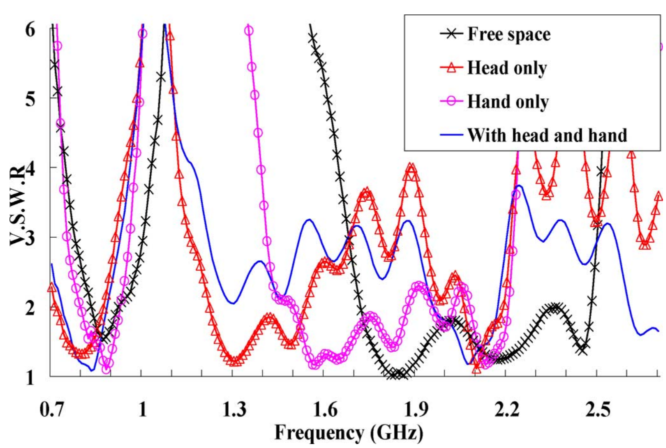

Fig. 7. Measured V.S.W.R against frequency of antenna with phantom-head and hand.

TABLE II
THE LIQUID PROPERTY OF PHANTOM-HEAD/HAND

Target frequency (MHz)	ε_r	σ (S/m)
835	30.3	0.59
900	30	0.62
1800	27	0.99
1900	26.7	1.04
1950	26.6	1.07
2000	26.5	1.09
2100	26.3	1.14
2450	25.7	1.32
ε_r = relative permittivity and σ= conductivity		

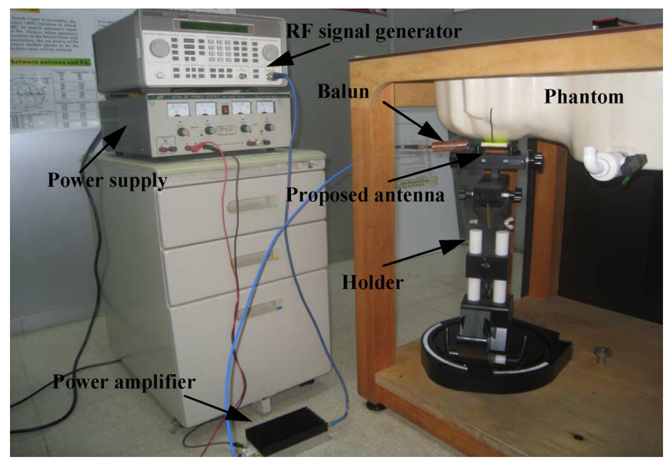

Fig. 8. Photo of experimental arrangement for SAR measurement.

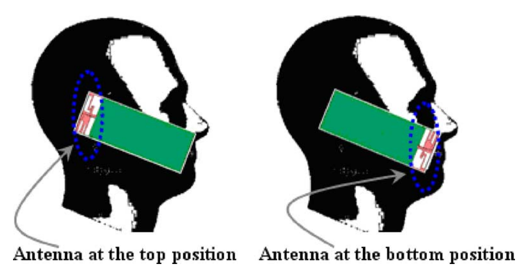

Fig. 9. The physical model for measuring SAR with the proposed antenna at the top and bottom position of the handset body.

B. Analysis of the SAR

The SAR in passive mode has been measured using Dasy-4 system [13], as shown in Fig. 8. The antenna is placed at the cheek position of the right-hand side of the phantom, and the spacing between the ground-plane and the cheek is 3 mm. Two cases for the proposed antenna test are shown in Fig. 9. The input power of the proposed antenna at GSM, CDMA and WCDMA bands is 24 dBm. However, the input power at DCS and PCS bands is 21 dBm (both considering a user channel being 1/8 of a time slot) [2]. The liquid parameters used in the measurements are listed in Table III. The measured SAR results in 1 g mass of simulated tissue from exposure to the antenna radiation are listed in Table IV. When the proposed antenna is to be located at the top position (normal using mode), it is seen that the 1 g mass SAR results at all frequencies meet the SAR limit of 1.6 mW/g. We can also observe that the difference between the measured SAR at the top and bottom positions is large. Obviously, this is due to the high current density concentration around the antenna. In general, the SAR passive test is only a preliminary measurement and the test results are used to analyze the antenna. In practical application, SAR is finally tested with an active device which may result in a different SAR value due to extra device elements.

TABLE III
THE LIQUID PROPERTY OF PHANTOM

Target frequency (MHz)	Head	
	ε_r	σ (S/m)
835	41.5	0.90
900	41.5	0.97
915	41.5	0.98
1800-2000	40	1.4
ε_r = relative permittivity and σ= conductivity		

TABLE IV
THE MEASURED SAR RESULTS IN 1-g OF THE SIMULATED TISSUE FROM EXPOSURE TO THE ANTENNA RADIATION WITH TWO CASES OF THE PROPOSED ANTENNA TO LOCATE AT THE TOP AND BOTTOM POSITIONS OF THE HANDSET BODY

Frequency (MHz)	Antenna at top position	Antenna at bottom position	SAR different value
	SAR_{1g} (mW/g)	SAR_{1g} (mW/g)	SAR_{1g} (mW/g)
850	1.49	0.69	0.8
902	1.53	0.78	0.75
1720	1.44	0.31	1.13
1920	1.43	0.41	1.02
2045	1.29	0.37	0.92

IV. CONCLUSION

In this communication, the proposed hexa-band antenna is practically capable to operate at the CDMA, GSM, DCS, PCS, WCDMA and Bluetooth bands. We demonstrated that a printed asymmetric T-type monopole with a solid shorting-line and a solid open-stub structure provides the hexa-band operation. By correctly choosing the shorting-line parameters and by modifying the shape of the T-type monopole arms, two bandwidths, 17.8% and 37.1%, can be obtained. The contribution of this communication is to implement a simple and low profile antenna for the practical mobile handset application. Measurement results show that a broad bandwidth is obtained. Although this antenna is designed for mobile handset applications, this design concept can be extended to the antenna design for laptop computers.

ACKNOWLEDGMENT

The authors would like to thank Prof. C.-Y. Wu (IEEE Life Fellow, Dept. of E.E, Jinwen University of Science and Technology), Prof. C.-W. Hsue (IEEE Fellow, Dept. of E.E, National Taiwan University of Science and Technology) for their help. The authors also appreciate the reviewer's comments to improve the quality of this communication.

REFERENCES

[1] Ramiro and Chaouki, "Wireless communications and networking: An overview," *IEEE Antennas Propag. Mag.*, vol. 44, pp. 185–193, Feb. 2002.

[2] C.-H. Chang and K.-L. Wong, "Printed $\lambda/8$-PIFA for penta-band WWAN operation in the mobile phone," *IEEE Trans. Antennas Propag.*, vol. 57, pp. 1373–1381, May 2009.

[3] J. D. Kraus and R. J. Marchefka, *Antennas*, 3rd ed. New York: Mc Graw-Hill, 2002, pp. 804–805.

[4] K.-L. Wong, G. Y. Lee, and T.-W. Chiou, "A low-profile planar monopole antenna for multiband operation of mobile handsets," *IEEE Trans. Antennas Propag.*, vol. 51, no. 1, pp. 121–125, Jan. 2003.

[5] Z. Li and Y. Rahmat-Samii, "Optimization of PIFA-IFA combination in handset antenna design," *IEEE Trans. Antennas Propag.*, vol. 53, pp. 1770–1777, May 2005.

[6] P. Vainikainen, J. Ollikainen, O. Kivekäs, and I. Kelander, "Resonator-based analysis of the combination of mobile handset antenna and chassis," *IEEE Trans. Antennas Propag.*, vol. 50, no. 10, pp. 1433–1444, Oct. 2002.

[7] A. Cabedo, J. Anguera, C. Picher, M. Ribó, and C. Puente, "Multi-band handset antenna combining a PIFA, slots, and ground plane modes," *IEEE Trans. Antennas Propag.*, vol. 57, no. 9, pp. 2526–2533, Sep. 2009.

[8] R. Hossa, A. Byndas, and M. E. Bialkowski, "Improvement of compact terminal antenna performance by incorporating open-end slots in ground plane," *IEEE Microw. Wireless Compon. Lett.*, vol. 14, no. 6, Jun. 2004.

[9] J. Anguera, I. Sanz, A. Sanz, A. Condes, D. Gala, C. Puente, and J. Soler, "Enhancing the performance of handset antennas by means of groundplane design," presented at the IEEE Int. Workshop on Antenna Technology: Small Antennas and Novel Metamaterials (iWAT 2006), New York, Mar. 2006.

[10] C. Picher, J. Anguera, A. Cabedo, C. Puente, and S. Kahng, "Multiband handset antenna using slots on the ground plane: Considerations to facilitate the integration of the feeding transmission line," *Progr. Electromagn. Res. C*, vol. 7, pp. 95–109, 2009.

[11] C.-M. Peng, I.-F. Chen, and C.-W. Hsue, "Modified printed folded $\lambda/8$ dipole antenna for DVB applications," *IEICE Trans. Commun.*., vol. E90-B, pp. 2991–2994, Oct. 2007.

[12] I.-F. Chen, C.-M. Peng, and S.-C. Liang, "Single layer printed monopole antenna for dual ISM-band operation," *IEEE Trans. Antennas Propag.*, vol. 53, no. 4, pp. 1270–1273, Apr. 2005.

[13] Schmid and Partner Engineering, AG (SPEAG) [Online]. Available: http://www.speag.com/speag/products.php